LETTER

doi:10.1038/nature11357

Oceanic nitrogen reservoir regulated by plankton diversity and ocean circulation

Thomas Weber[1] & Curtis Deutsch[1]

The average nitrogen-to-phosphorus ratio of marine phytoplankton (16N:1P) is closely matched to the nutrient content of mean ocean waters (14.3N:1P). This condition is thought to arise from biological control over the ocean's nitrogen budget, in which removal of bioavailable nitrogen by denitrifying bacteria ensures widespread selection for diazotrophic phytoplankton that replenish this essential nutrient when it limits the growth of other species[1–3]. Here we show that in the context of a realistic ocean circulation model, and a uniform N:P ratio of plankton biomass, this feedback mechanism yields an oceanic nitrate deficit more than double its observed value. The critical missing phenomenon is diversity in the metabolic N:P requirement of phytoplankton, which has recently been shown to exhibit large-scale patterns associated with species composition[4]. When we model these variations, such that diazotrophs compete with high N:P communities in subtropical regions, the ocean nitrogen inventory rises and may even exceed the average N:P ratio of plankton. The latter condition, previously considered impossible, is prevented in the modern ocean by shallow circulations that communicate stoichiometric signals from remote biomes dominated by diatoms with low N:P ratios. Large-scale patterns of plankton diversity and the circulation pathways connecting them are thus key factors determining the availability of fixed nitrogen in the ocean.

The biologically mediated feedback between marine denitrification and N_2 fixation operates like a 'nutrient thermostat'[1,2,5] that couples the ocean's fixed N reservoir (primarily in the form of nitrate, NO_3^-) to its less dynamic reservoir of P (primarily phosphate, PO_4^{3-}). A central element of this self-regulating mechanism is the partition of ecological niches between diazotrophic (N_2-fixing) phytoplankton, which grow slowly but do not require an external supply of fixed N (refs 6, 7), and other plankton that grow quickly but are often N-limited owing to persistent N removal in anoxic environments[8–10]. The quantitative understanding of this mechanism rests on box models, in which diazotrophs maintain the ocean's ratio of major nutrient reservoirs ($\Sigma N/\Sigma P$) close to, but slightly below, the N:P requirements of the plankton with which they compete for PO_4^{3-} (refs 5, 11, 12).

Box model depictions make two major simplifications. First, diazotrophs are assumed to compete with plankton having a universal Redfield ratio of 16N:1P, which sets a threshold for N_2 fixation and constitutes the 'set point' of the nutrient thermostat, towards which $\Sigma N/\Sigma P$ is restored. In reality, the Redfield ratio is only an average value and plankton N:P varies systematically between marine species and their preferred biomes[4,13–15]. It has thus been hypothesized that the regulation of $\Sigma N/\Sigma P$ is biased towards the nutrient requirements of those species cohabiting with diazotrophs in subtropical biomes[3]. Second, the circulation pathways that transport nutrients between surface regions with different species composition and N:P ratios are not represented in box models, but may have a central role in shaping the ecological niche of diazotrophs[3]. A realistic physical model is required to identify the processes maintaining the N reservoir of an ocean with diverse plankton stoichiometry.

We developed a simple ecosystem and biogeochemical model to simulate the long-term coupling of N and P cycles in an observationally constrained ocean general circulation model (GCM). The ecosystem comprises a general phytoplankton class (O) that assimilates NO_3^- and PO_4^{3-} in the molar ratio R_O, and a diazotrophic class (F) that assimilates PO_4^{3-} and releases NO_3^- from newly fixed N_2. The maximum growth rate of N_2-fixers (μ_F) is reduced relative to that of other phytoplankton (μ_O), to reflect a constant energetic cost of diazotrophy and a variable dependence on iron (Fe)[16,17]. Fe-limitation is patterned according to the distribution of atmospheric dust deposition, and its overall strength is varied between simulations (Fig. 1a, Supplementary Fig. 1). Denitrification is simulated in benthic grid boxes and anoxic regions of the water column (Supplementary Fig. 2), and its global rate is also varied within specified limits. The model's P reservoir is conserved at the modern ocean value, but its N inventory adjusts over millennial timescales until a steady-state balance between N_2-fixation and denitrification is achieved. See Methods for model details.

Consistent with box models[5], we found that in a 'Redfieldian' ocean where $R_O = 16$ everywhere, the steady-state value of $\Sigma N/\Sigma P$ depends on two parameters: (1) the globally integrated rate of denitrification, and (2) the competitive handicap faced by diazotrophs (μ_F/μ_O). The decrease in $\Sigma N/\Sigma P$ at higher denitrification rates and stronger Fe limitation (Fig. 1b) reflects the proportions of PO_4^{3-} and NO_3^- required to support global N_2 fixation rates that balance N removal through denitrification. Because diazotrophs have slow growth rates, they compete successfully for PO_4^{3-} only when NO_3^- is low enough to hinder their competitors to a similar degree. The diazotrophic niche is thus determined, through competitive dynamics, by the NO_3^-: PO_4^{3-} ratio of ambient sea water, even though their growth is explicitly independent of NO_3^-. When strong Fe limitation exacerbates their competitive handicap, the deep ocean must accumulate a larger deficit of NO_3^- (lower $\Sigma N/\Sigma P$) to support the required N_2-fixation rate. Similarly, higher global rates of denitrification must be balanced by enhanced N_2 fixation that, for a given diazotrophic growth rate, can only be achieved with a greater excess of PO_4^{3-} (lower $\Sigma N/\Sigma P$).

Throughout the observationally supported range of global denitrification rates (150–250 teragrams of N per year, Tg N yr^{-1}, ref. 18), simulated $\Sigma N/\Sigma P$ is considerably lower than its observed value of approximately 14.3. For the average plankton, this amounts to a global deficit of NO_3^- relative to PO_4^- of 6–13 μM, which is 2–4 times larger than observed. Even when Fe limitation is eliminated, unrealistically low denitrification rates (<100 Tg N yr^{-1}) are required to reconcile the model with observations (Fig. 1b). Neither a shift in the patterns of denitrification nor greater model complexity—adding dissolved organic matter, a complete iron cycle, or minor N budget terms—can eliminate this discrepancy (see Supplementary Notes). It can only be resolved by expanding the ecological niche of diazotrophs. This cannot be accomplished by increasing their growth rate, which already reaches near parity with other plankton. It requires a process through which the availability of PO_4^{3-} is enhanced relative to NO_3^- in the subtropics. We investigated whether large-scale deviations from

[1]University of California Los Angeles, Los Angeles, California 90095, USA.

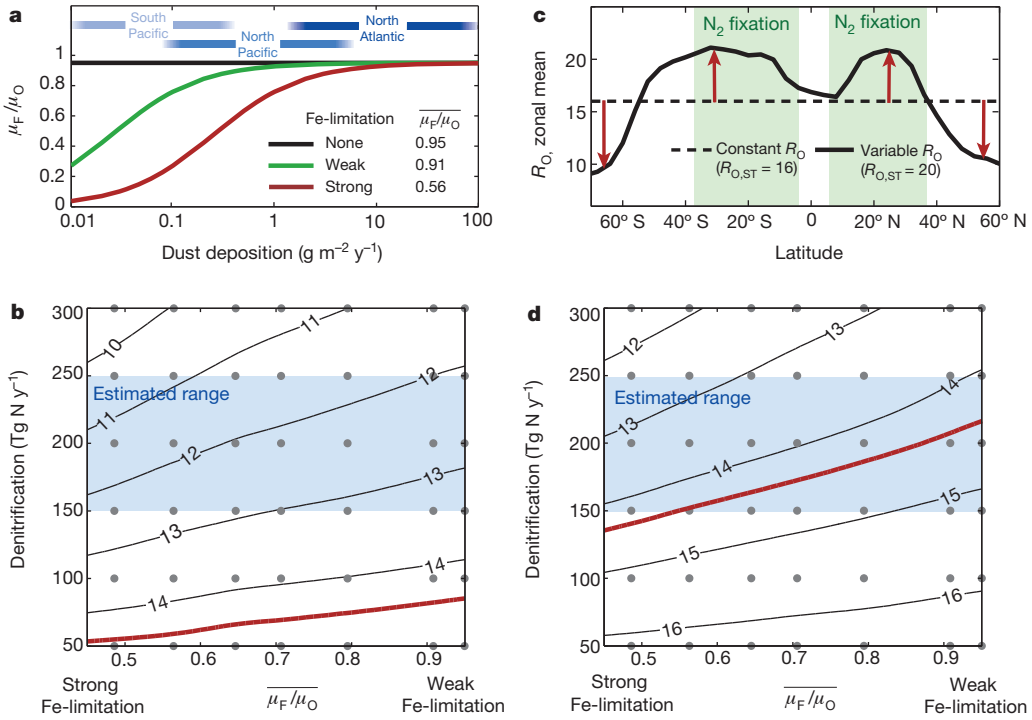

Figure 1 | Model scenarios and solutions. **a**, Growth rate of diazotrophs relative to other phytoplankton, as a function of atmospheric dust deposition. When Fe limitation is stronger, μ_F/μ_O is more variable between regions of high and low deposition, and its mean value ($\overline{\mu_F/\mu_O}$) is reduced. **b**, Predicted steady-state ΣN/ΣP (black contours) for a Redfieldian ocean, across a range of denitrification and Fe-limitation scenarios. Blue shading represents observational constraints on denitrification range; red line indicates observed ΣN/ΣP; grey dots are solutions of individual simulations. **c**, Variations in R_O are incorporated using inferred community composition. Diazotrophs are predominantly confined to the green-shaded latitude bands. **d**, As for **b**, except for stoichiometrically diverse scenarios ($R_{O,ST} \approx 20$).

Redfield stoichiometry in nutrient uptake by non-fixing phytoplankton[3] could provide such a mechanism, and resolve the gap between model predictions and measurements.

Large-scale variations in R_O have recently been shown to hold throughout the Southern Ocean, where polar latitudes dominated by diatoms export low N:P organic matter, while Subantarctic latitudes are characterized by high N:P export ratios[4]. We added stoichiometric diversity to the plankton in our model by extending this empirically derived relationship between plankton biogeography and biomass N:P (see Methods), while ensuring a global mean nutrient export ratio of 16N:1P (Fig. 1c, Supplementary Figs 3 and 4). Because diatoms are abundant in equatorial and high latitudes but scarce in the subtropics, the mean N:P of plankton that compete directly with diazotrophs—denoted $R_{O,ST}$—is close to 20. This is consistent with the elemental composition of the cyanobacteria that dominate oligotrophic waters[19,20], the observed N:P of organic matter in the North Pacific Subtropical Gyre[21], and theoretical predictions of high N:P allocation strategies during resource competition[22].

The introduction of stoichiometric diversity allows the model to achieve the observed ΣN/ΣP values across a wide range of plausible denitrification and Fe-limitation scenarios (Fig. 1d). This increase is driven by the high N:P requirements of oligotrophic phytoplankton, which exacerbates N limitation in the subtropical gyres. A larger excess of PO_4^{3-} then remains to fuel N_2 fixation, expanding the niche of diazotrophs beyond that created by subsurface denitrification. This allows a balanced N budget to be achieved at higher values of ΣN/ΣP. Under weak Fe limitation and low denitrification rates, ΣN/ΣP actually exceeds the average N:P of marine plankton (Fig. 1d)—a condition that cannot be attained in previous box-model depictions. The ocean's ratio of nutrient reservoirs thus depends not only on the mean N:P of its plankton, but also on their stoichiometric diversity.

To investigate the sensitivity of ΣN/ΣP to different levels of stoichiometric diversity, we varied the N:P quota of diatom and non-diatom endmember communities, while maintaining a constant average export ratio of 16N:1P. As plankton stoichiometry becomes more diverse, global ΣN/ΣP rises steadily (Fig. 2), reflecting the expansion of the diazotrophic niche caused by the high N:P requirements of plankton cohabiting subtropical regions (increased $R_{O,ST}$). However, for every increase in $R_{O,ST}$, the increase in ΣN/ΣP is only 40% as large, much less than would be required for diazotrophs to keep ΣN/ΣP in line with the needs of their local competitors. This implies that the ecological niche of diazotrophs is determined not only by local competition with high N:P plankton, but also by remote diatom-dominated communities with a lower N:P quota. These communities largely occupy different ocean biomes, so their stoichiometric signatures must be communicated over long distances by ocean circulation.

To illustrate the role of circulation in controlling ΣN/ΣP, we employ a three-box model[12] (Fig. 3a) in which the circulations that transport

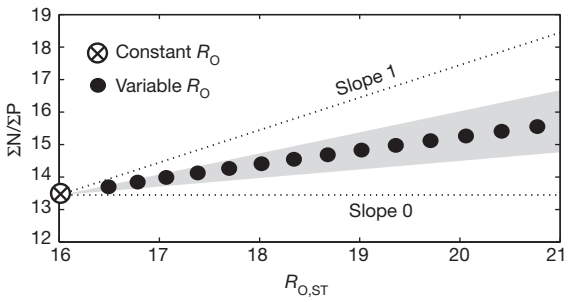

Figure 2 | Response of ΣN/ΣP to the degree of stoichiometric diversity, $R_{O,ST}$. Each simulation has 150 Tg N yr^{-1} denitrification and no Fe limitation. If the 'set point' of the nutrient thermostat were determined through local competition only, ΣN/ΣP would rise with $R_{O,ST}$ along a line of slope 1, yet a much weaker response is observed in our model. Grey shading represents an estimate of error for the slope of this line, derived using different estimates of diatom abundance as the basis for R_O (see Methods and Supplementary Notes).

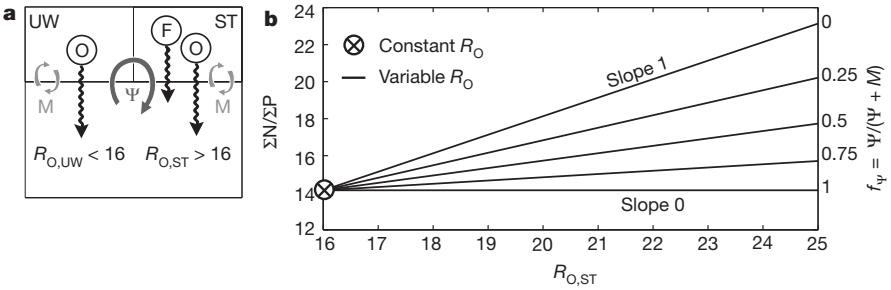

Figure 3 | Role of ocean circulation illustrated in a three-box model. **a**, Structure of the model, with two surface regions (upwelling UW; subtropics ST) and two circulation pathways (vertical exchange M; overturning Ψ). Diazotrophs are restricted to ST, and other plankton have diverse stoichiometry, which we vary by raising $R_{O,ST}$ and reducing $R_{O,UW}$ to maintain a mean of 16. **b**, The response of ΣN/ΣP to stoichiometric diversity depends on $f_Ψ$, the fraction of subtropical source waters that first pass through UW.

nutrients between the surface and deep ocean, and between diatom-dominated upwelling regions (UW) and downwelling subtropical gyres (ST), can be abstracted and manipulated (see Methods). When surface nutrients are supplied only from vertical exchange (M) with the deep ocean, the niche of diazotrophs is governed by their local competitors only, so every change in $R_{O,ST}$ produces an equal change in ΣN/ΣP, even though the global mean R_O is anchored at 16 (Fig. 3b, $f_Ψ = 0$). However, when the nutrients are predominantly supplied through shallow overturning and near-surface lateral circulations (Ψ), the signature of low N:P uptake—a higher residual NO_3^-:PO_4^{3-} ratio in surface waters—is transported directly from diatom-dominated upwelling regions into the subtropics. This reduces the excess PO_4^{3-} available to diazotrophs, and must be compensated by lower NO_3^-: PO_4^{3-} in upwelling deep water to maintain a given N_2-fixation rate. The response of the ocean's ΣN/ΣP to increases in $R_{O,ST}$ is thus damped as lateral circulations strengthen relative to vertical exchange. In the extreme case where all subtropical nutrients pass first through surface communities with low N:P ratios (Fig. 3b, $f_Ψ = 1$), the ocean N reservoir is entirely independent of spatial variations in R_O, and ΣN/ΣP is regulated through the global-mean N:P of plankton, as originally hypothesized by Redfield[1].

In light of these box model results, the tendency of ΣN/ΣP in the GCM to track only about 40% of a change in $R_{O,ST}$ (Fig. 2) suggests that about half the waters reaching subtropical sites of N_2-fixation are first influenced by low N:P plankton communities outside the subtropics. The dependence of global ΣN/ΣP on the spatial pattern of plankton N:P ratios can be computed by introducing taxon-dependent deviations from a constant-Redfield N:P (Fig. 1c, Supplementary Fig. 4) one grid cell at a time (see Methods). Regions can be divided between those whose stoichiometric deviations tend to raise ΣN/ΣP compared to the Redfieldian case (reddish positive values, Fig. 4a), and those that tend to reduce it (bluish negative values, Fig. 4a). Large negative values are found in the northern and equatorial Pacific and, to a lesser extent, in the polar regions of the Southern Ocean. The transport of nutrients from these source regions into the subtropics, through surface Ekman currents and shallow overturning, creates a 'biogeochemical teleconnection' by which remote low N:P communities reduce the availability of PO_4^{3-} to fuel N_2 fixation. This counteracts the expanded niche of diazotrophs produced by local competition with high-N:P subtropical communities, offsetting roughly half of the upwards pressure on ΣN/ΣP (Fig. 4b). Ocean circulation thus plays a critical role in the nutrient thermostat, reducing the bias of ΣN/ΣP towards the stoichiometry of subtropical communities, and holding the nutrient content of sea water closer to the global average requirements of phytoplankton.

The ratio of oceanic N and P reservoirs is a simple but powerful observational constraint on the dynamics of the marine N cycle. It appears to be fundamentally incompatible with a universal Redfield ratio of plankton biomass, lending global support to the large-scale association between biogeography and plankton nutrient metabolism inferred from Southern Ocean nutrient data[4].

The modern ocean's ΣN/ΣP also places new bounds on global denitrification rates and the limitations to diazotroph growth. Denitrification rates at the upper end of the estimated range (>250 Tg N yr^{-1}) are unable to yield the observed ΣN/ΣP ratio, even with a high degree of stoichiometric diversity (Fig. 1d). At the same time, the net effect of stoichiometric diversity among plankton taxa is to expand the ecological niche of marine diazotrophs. In geochemical estimates of N_2 fixation based on surface nutrients[23,24], this would translate into higher diagnosed N_2-fixation rates in the subtropics, not lower rates[24]. Thus, stoichiometric diversity helps to close the long-standing gap between estimates of N sources and sinks[25].

From a mechanistic perspective, the expanded niche for diazotrophs yields a higher ΣN/ΣP for a given denitrification rate, but this is still insufficient to achieve observed ΣN/ΣP when diazotrophs are strongly limited by airborne Fe (Fig. 1d). At most, the overall growth-rate handicap of diazotrophs can approach 50%, and then only if denitrification rates are at the lower end of the estimated range. If the intrinsic cost of diazotrophy were greater than the conservative value we use ($μ_F/μ_O = 0.95$), or if diazotroph growth is also slowed by

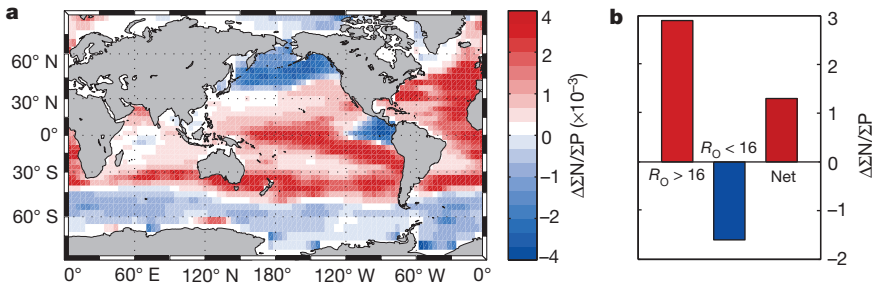

Figure 4 | Influence of individual surface regions on ΣN/ΣP. **a**, Values of ΔΣN/ΣP represent the change in steady-state ΣN/ΣP (from the Redfield case) prompted by introducing the grid cell's deviation of R_O from 16 (Supplementary Fig. 4), while holding $R_O = 16$ elsewhere (see Methods). **b**, Integral of ΔΣN/ΣP over regions of high R_O (>16) and low R_O (<16), and over the entire global domain ('Net'). High- and low-R_O regions exert opposite pressures on the ocean N reservoir, with a net increase in ΣN/ΣP over the Redfield case.

other factors not included here[6], then the observed ΣN/ΣP would require even weaker Fe limitation (see Supplementary Notes). These findings imply a secondary role for atmospheric Fe deposition in controlling rates of N_2 fixation in the modern ocean.

Temporal changes in the mean N:P of plankton have been hypothesized to drive long-term trends in ocean fertility and carbon storage, by shifting the set point of its nutrient thermostat[26,27]. Our model shows that this set point is also controlled by the biogeography of distinct plankton taxa, and ocean circulation patterns that transport nutrients between biomes—two factors known to vary with climatic conditions. Future stratification of the upper ocean and the expansion of oligotrophic biomes expected under a warming climate[28] could reshape the ecological niche of diazotrophs, and initiate a long-term perturbation in the ocean's nutrient thermostat.

METHODS SUMMARY

We used an observationally constrained ocean GCM (ref. 29) with horizontal resolution of $4^\circ \times 4^\circ$ and 24 vertical layers, and simulated tracer transport using the transport matrix method[30]. A simple ecosystem model was adopted from refs 5 and 12, but modified for a three-dimensional global domain. The model includes four prognostic variables: NO_3^-, PO_4^{3-}, 'general' phytoplankton, and diazotrophic phytoplankton. Plankton growth rates vary as a function of temperature, light, and nutrient concentrations, and the parameters governing these relationships were tuned to optimize surface nutrient distributions (Supplementary Fig. 5). Diazotroph growth rates are scaled by atmospheric dust deposition to represent a heightened requirement for Fe in maintaining the nitrogenase enzyme. The strength of this scaling is varied to simulate differing degrees of Fe limitation. The spatial pattern of denitrification is governed by the degradation of organic matter in benthic grid cells and those where observed oxygen concentrations fall below 5 μM. The fluxes are then scaled in order to vary the global rate of N loss in a controlled manner between model scenarios. Each simulation was initialized with observed nutrient distributions and integrated for at least 10,000 years, until the N budget was balanced to within 0.1 Tg N yr^{-1}. Stoichiometric diversity among phytoplankton was parameterized using observed distributions of silicic acid to estimate the contribution of diatoms to nutrient export, and assuming different biomass N:P ratios for diatoms and other non-diazotrophic taxa. For each simulation, the value of $R_{O,ST}$ was calculated as the mean N:P ratio of plankton communities cohabiting surface grid boxes with diazotrophs at steady state.

Full Methods and any associated references are available in the online version of the paper.

Received 5 November 2011; accepted 27 June 2012.

1. Redfield, A. C. The biological control of chemical factors in the environment. *Am. Sci.* **46,** 205–221 (1958).
2. Redfield, A. C., Ketchum, B. H. & Richards, F. A. in *The Sea* Vol. 2 (ed. Hill, M. N.) 26–77 (Interscience, 1963).
3. Deutsch, C. & Weber, T. Nutrient ratios as a tracer and driver of ocean biogeochemistry. *Annu. Rev. Mar. Sci.* **4,** 113–141 (2012).
4. Weber, T. S. & Deutsch, C. Ocean nutrient ratios governed by plankton biogeography. *Nature* **467,** 550–554 (2010).
5. Tyrrell, T. The relative influences of nitrogen and phosphorus on oceanic primary production. *Nature* **400,** 525–531 (1999).
6. Karl, D. *et al.* Dinitrogen fixation in the world's oceans. *Biogeochemistry* **57/58,** 47–98 (2002).
7. Capone, D. G., Zehr, J. P., Paerl, H. W., Bergman, B. & Carpenter, E. J. Trichodesmium, a globally significant marine cyanobacterium. *Science* **276,** 1221–1229 (1997).
8. Codispoti, L. A. in *Productivity of the Ocean: Past and Present* (eds Berger, W. H., Smetacek, V. S. & Wefer, G.) 377–394 (John Wiley and Sons, 1989).
9. Ward, B. B. *et al.* Denitrification as the dominant nitrogen loss process in the Arabian Sea. *Nature* **461,** 78–81 (2009).
10. Lam, P. & Kuypers, M. M. M. Microbial nitrogen cycling processes in oxygen minimum zones. *Annu. Rev. Mar. Sci.* **3,** 317–345 (2011).
11. Lenton, T. M. & Watson, A. J. Redfield revisited. 1. Regulation of nitrate, phosphate, and oxygen in the ocean. *Glob. Biogeochem. Cycles* **14,** 225–248 (2000).
12. Lenton, T. M. & Klausmeier, C. A. Biotic stoichiometric controls on the deep ocean N: P ratio. *Biogeosciences* **4,** 353–367 (2007).
13. Quigg, A. *et al.* The evolutionary inheritance of elemental stoichiometry in marine phytoplankton. *Nature* **425,** 291–294 (2003).
14. Green, S. E. & Sambrotto, R. N. Plankton community structure and export of C, N, P and Si in the Antarctic Circumpolar Current. *Deep Sea Res. II* **53,** 620–643 (2006).
15. Arrigo, K. R. *et al.* Phytoplankton community structure and the drawdown of nutrients and CO_2 in the Southern Ocean. *Science* **283,** 365–367 (1999).
16. Berman-Frank, I., Cullen, J. T., Shaked, Y., Sherrell, R. M. & Falkowski, P. G. Iron availability, cellular iron quotas, and nitrogen fixation in *Trichodesmium*. *Limnol. Oceanogr.* **46,** 1249–1260 (2001).
17. Kustka, A., Carpenter, E. J. & Sanudo-Wilhelmy, S. A. Iron and marine nitrogen fixation: progress and future directions. *Res. Microbiol.* **153,** 255–262 (2002).
18. DeVries, T., Deutsch, C., Primeau, F., Chang, B. & Devol, A. Global rates of water-column denitrification derived from nitrogen gas measurements. *Nature Geosci.* **5,** 547–550 (2012).
19. Heldal, M., Scanlan, D. J., Norland, S., Thingstad, F. & Mann, N. H. Elemental composition of single cells of various strains of marine *Prochlorococcus* and *Synechococcus* using X-ray microanalysis. *Limnol. Oceanogr.* **48,** 1732–1743 (2003).
20. Bertilsson, S., Berglund, O., Karl, D. M. & Chisholm, S. W. Elemental composition of marine *Prochlorococcus* and *Synechococcus*: implications for the ecological stoichiometry of the sea. *Limnol. Oceanogr.* **48,** 1721–1731 (2003).
21. Karl, D. M. *et al.* Ecological nitrogen-to-phosphorus stoichiometry at station ALOHA. *Deep Sea Res. II* **48,** 1529–1566 (2001).
22. Klausmeier, C. A., Litchman, E., Daufresne, T. & Levin, S. A. Optimal nitrogen-to-phosphorus stoichiometry of phytoplankton. *Nature* **429,** 171–174 (2004).
23. Deutsch, C., Sarmiento, J. L., Sigman, D. M., Gruber, N. & Dunne, J. P. Spatial coupling of nitrogen inputs and losses in the ocean. *Nature* **445,** 163–167 (2007).
24. Mills, M. M. & Arrigo, K. R. Magnitude of oceanic nitrogen fixation influenced by the nutrient uptake ratio of phytoplankton. *Nature Geosci.* **3,** 412–416 (2010).
25. Codispoti, L. A. Biogeochemical cycles—is the ocean losing nitrate? *Nature* **376,** 724 (1995).
26. Falkowski, P. G. Rationalizing elemental ratios in unicellular algae. *J. Phycol.* **36,** 3–6 (2000).
27. Broecker, W. S. & Henderson, G. M. The sequence of events surrounding Termination II and their implications for the cause of glacial-interglacial CO_2 changes. *Paleoceanography* **13,** 352–364 (1998).
28. Polovina, J. J., Howell, E. A. & Abecassis, M. Ocean's least productive waters are expanding. *Geophys. Res. Lett.* **35,** L03618 (2008).
29. DeVries, T. & Primeau, F. Dynamically and observationally constrained estimates of water-mass distributions and ages in the global ocean. *J. Phys. Oceanogr.* **41,** 2381–2401 (2011).
30. Khatiwala, S. A computational framework for simulation of biogeochemical tracers in the ocean. *Glob. Biogeochem. Cycles* **21,** doi:10.1029/2007GB002923 (2007).

Supplementary Information is linked to the online version of the paper at www.nature.com/nature.

Acknowledgements We thank T. DeVries for providing the ocean circulation model. This work was funded by a NASA Earth Systems Science Fellowship (T.W.) and a grant from the Gordon and Betty Moore Foundation (C.D.).

Author Contributions T.W. developed the model and performed simulations and analyses. Both authors designed the study and wrote the paper.

Author Information Reprints and permissions information is available at www.nature.com/reprints. The authors declare no competing financial interests. Readers are welcome to comment on the online version of this article at www.nature.com/nature. Correspondence and requests for materials should be addressed to T.W. (tweber@atmos.ucla.edu).

METHODS

Circulation model. We use an observationally constrained ocean GCM which optimizes circulation to fit the linearized momentum equations, and observed distributions of temperature and salinity, and ^{14}C (ref. 29). It has horizontal resolution of $4^\circ \times 4^\circ$, and 24 vertical layers including two in the top 75 m. Annual-mean flow fields are extracted as a matrix, $\boldsymbol{A}$, facilitating tracer simulations using the transport matrix method[30].

Ecosystem model. We adopt a simple ecosystem model (similar to refs 5 and 12) that includes four prognostic variables, representing the concentrations (in μM) of NO_3^- (N), PO_4^{3-} (P), 'general' phytoplankton (O), and diazotrophic phytoplankton (F). Both phytoplankton types are simulated as organic phosphorous pools. The variables are governed by:

$$\frac{dO}{dt} = \mu_O \min\left(\frac{P}{P+K_P}, \frac{N}{N+K_N}\right) O - MO \quad (1)$$

$$\frac{dF}{dt} = \mu_F \frac{P}{P+K_P} F - MF \quad (2)$$

$$\frac{dP}{dt} = AP - (J_{O,UP} + J_{F,UP}) + Q_{rem}(M(O+F)) \quad (3)$$

$$\frac{dN}{dt} = AN - R_O J_{O,UP} + Q_{rem}(M(R_O O + R_F F)) - D \quad (4)$$

The parameters of the ecosystem model are discussed below and their numeric values listed in Supplementary Table 1.

Growth and mortality. The first terms on the right hand side of equations (1) and (2) represent plankton growth, as a function of environmental factors. The maximum growth rate of O (μ_O) is given by:

$$\mu_O(T,I) = \mu_{opt} \exp(k(T-T'))(1 - \exp(-I/K_I)) \quad (5)$$

Here, μ_{opt} is the growth rate under optimal conditions, and k, T', K_I, K_P and K_N control the sensitivity of growth to temperature (T), light (I) and nutrient concentrations. Sensitivity parameters are tuned to reproduce observed surface nutrient distributions[31] in the model, ensuring a realistic pattern of biological nutrient drawdown (Supplementary Fig. 5). We account for the competitive handicap of diazotrophs by reducing their maximum growth rate (μ_F) relative to general plankton. It is scaled by a constant factor (δ_F), representing an intrinsic energetic expenditure on nitrogenase activity, and by a Fe-limitation parameter to represent the heightened requirement by diazotrophs for Fe:

$$\mu_F(T,I,Fe) = \mu_O \delta_F \frac{J_{Fe}}{J_{Fe}+K_{Fe}} \quad (6)$$

J_{Fe} is the simulated distribution of atmospheric Fe deposition onto the surface ocean[32], and the strength of the Fe-limitation is varied through K_{Fe} (Supplementary Fig. 1). In equations (1) and (2), M represents phytoplankton mortality, and includes a quadratic term that scales with total biomass ($M = m_1 + m_2 B$, where $B = O + F$, and m_1 and m_2 are rate constants) and can be thought of as representing grazing by zooplankton, which are not explicitly simulated.

Nutrient cycling. Nutrients are transported by the circulation operator (matrix $\boldsymbol{A}$), and are assimilated into biological pools in the top 75 m through plankton growth. In equations (3) and (4), $J_{O,UP}$ and $J_{F,UP}$ are the same as the first terms on the right hand side of equations (1) and (2) respectively. R_O is the biomass N:P ratio of general phytoplankton, and R_F is the amount of N fixed per unit P uptake by diazotrophs. Following phytoplankton mortality, the recycling and remineralization of organic matter is simulated using the operator Q_{rem}. The majority is recycled in the surface ocean, and restored to local inorganic pools. A small fraction (ϕ_e) is exported from the surface layers as organic particles, and remineralized over depth following a power-law relation[33].

N budget. Newly fixed N is assumed to derive from an abundant dissolved N_2 pool that is not simulated explicitly. In equation (4), D represents the sum of water-column and sediment denitrification, which are simulated as sinks of NO_3^-. Water-column denitrification is proportional to the remineralization rate of organic matter in grid cells with climatological oxygen concentrations below a critical threshold $[O_2]_{crit}$. Sediment denitrification is determined by the flux of organic matter to seafloor grid cells[34]. Because global denitrification rates are one of the primary determinants of the steady-state N inventory, but are not well constrained observationally, D is scaled to maintain a specified global rate, and a constant partition among water column and sediments, thus controlling for these factors between simulations. Simulated distributions of N sources and sinks are shown in Supplementary Fig. 2.

Plankton N:P ratios. We assume that stoichiometric variability occurs primarily at the taxonomic level, and use the empirical relation derived by ref. 4:

$$R_O = R_{O,diat}\phi_{diat} + R_{O,other}(1-\phi_{diat}) \quad (7)$$

Here, ϕ_{diat} is the fractional contribution of diatoms to nutrient export, and $R_{O,diat}$ and $R_{O,other}$ are the biomass N:P ratios of diatoms and other non-diazotropic phytoplankton respectively. Rather than simulate different taxonomic groups explicitly, we use a prior estimate of ϕ_{diat} combined with equation (7) to apply a spatially varying pattern of R_O to the single class of non-diazotrophic plankton. Three different approaches are considered for estimating ϕ_{diat} (Supplementary Fig. 3). Method 1 assumes that the relative abundance of diatoms scales with the observed surface concentration of $Si(OH)_4$ (ref. 35):

$$\phi_{diat} = \frac{[Si]}{[Si]+K_{Si}} \quad (8)$$

K_{Si} is tuned to accommodate the observational constraint that diatoms contribute 40–50% of global export production[36]. Methods 2 and 3 compute ϕ_{diat} from the relative export fluxes of N and Si and an estimate of the Si:N ratios in diatom biomass[37]. Method 2 is based on observations only[38], diagnosing export fluxes from the vertical gradients of Si and N between the thermocline and surface, whereas Method 3 diagnoses the fluxes in an ocean GCM[36]. We note that the two diagnostic methods are less appropriate in regions where N_2 fixation confounds the diagnosis of N export. We used the simplest approach (Method 1), which agrees most closely with satellite-derived estimates of diatom biogeography[39]. Methods 2 and 3 are used to derive an estimate of uncertainty associated with the community-composition parameterization.

In our initial simulations (Fig. 1), $R_{O,diat}$ and $R_{O,other}$ are held close to the values diagnosed in ref. 4, with the added constraint that the mean N:P export ratio by non-fixing plankton is equal to the Redfield ratio of 16:1 (Supplementary Fig. 4). In later simulations (Fig. 2), we vary $R_{O,diat}$ and $R_{O,other}$ to produce different degrees of stoichiometric diversity, but again ensure the global-mean constraint is satisfied. This allows us to identify changes in $\Sigma N/\Sigma P$ that are caused only by changes in the spatial pattern of R_O, and not its global-mean value. The ratio of N_2 fixation to P uptake by diazotrophs (R_F) is assumed to be constant, but as in previous studies[12], our results are not sensitive to the value of this parameter.

Sensitivity testing. We rigorously tested the sensitivity of our results to parameters and assumptions of the ecosystem model. See Supplementary Notes, Supplementary Figs 7–10 and Supplementary Table 2.

Three-box model. We use a three-box model of the ocean to assist our interpretation of the ocean GCM results. The geometry and nutrient fluxes of the model are shown in Supplementary Fig. 6. Its ecosystem and biogeochemistry components are held as close to the ocean GCM version as possible for ease of comparison, with the following simplifications:

(1) Phytoplankton growth rates are set to the optimal value in ST, and reduced by a factor of 0.5 in the UW, so that residual nutrients remain in the surface as observed.

(2) The competitive handicap of diazotrophs is determined only by δ_F in ST (no Fe limitation), and μ_F is set to zero in UW.

(3) Denitrification is distributed between the surface and deep ocean as in ref. 5.

Regional control of ΣN/ΣP. For each surface grid cell (with x,y coordinates i,j), a simulation was conducted in which the local R_O was set to its stoichiometrically diverse value, as computed from ϕ_{diat} (Supplementary Fig. 4). In all other surface regions, R_O was held equal to the Redfield ratio. The difference between the steady-state $\Sigma N/\Sigma P$ in this simulation, and that in a uniform Redfieldian case, was then computed:

$$\Delta\Sigma N/\Sigma P|_{\substack{x=i\\y=j}} = \frac{\Sigma N}{\Sigma P}\left(\begin{cases} R_O = f(\phi_{diat}), x=i, y=j \\ R_O = 16, x\neq i, y\neq j \end{cases}\right) - \frac{\Sigma N}{\Sigma P}(R_O = 16) \quad (9)$$

This value is taken as a measure of the sensitivity of $\Sigma N/\Sigma P$ to the uptake stoichiometry of plankton communities in the perturbed surface region. The efficiency of these computations was enhanced using a quasi-steady-state assumption for the 'fast' biological variables O and F, which reduces the model to a two-equation system that can be solved directly for steady state using Newton's method[40]. Sensitivity testing demonstrated that the solutions derived from the quasi-steady-state-assumption approach and full four-equation model were almost indistinguishable.

31. Garcia, H. E., Locarni, R. A., Boyer, T. P. & Antonov, J. I. *World Ocean Atlas 2005* Vol. 4 *Nutrients (phosphate, nitrate, silicate)* (US Government Printing Office, 2006).
32. Mahowald, N. M. *et al.* Change in atmospheric mineral aerosols in response to climate: last glacial period, preindustrial, modern, and doubled carbon dioxide climates. *J. Geophys. Res.* **111,** doi:10.1029/2005JD006653 (2006).

33. Martin, J. H., Gordon, R. M., Fitzwater, S. & Broenkow, W. W. VERTEX: phytoplankton/iron studies in the Gulf of Alaska. *Deep-Sea Res.* **36,** 649–680 (1989).
34. Middelburg, J. J., Soetaert, K., Herman, P. M. J. & Heip, C. H. R. Denitrification in marine sediments: a model study. *Glob. Biogeochem. Cycles* **10,** 661–673 (1996).
35. Egge, J. K. & Aksnes, D. L. Silicate as regulating nutrient in phytoplankton competition. *Mar. Ecol. Prog. Ser.* **83,** 281–289 (1992).
36. Jin, X., Gruber, N., Dunne, J. P., Sarmiento, J. L. & Armstrong, R. A. Diagnosing the contribution of phytoplankton functional groups to the production and export of particulate organic carbon, $CaCO_3$, and opal from global nutrient and alkalinity distributions. *Glob. Biogeochem. Cycles* **20,** doi:10.1029/2005GB002532 (2006).
37. Brzezinski, M. A. *et al.* A switch from $Si(OH)_4$ to NO_3-depletion in the glacial Southern Ocean. *Geophys. Res. Lett.* **29,** 1564 (2002).
38. Sarmiento, J. L. & Gruber, N. *Ocean Biogeochemical Dynamics* (Princeton University Press, 2006).
39. Alvain, S., Moulin, C., Dandonneau, Y. & Loisel, H. Seasonal distribution and succession of dominant phytoplankton groups in the global ocean: a satellite view. *Glob. Biogeochem. Cycles* **22,** doi:10.1029/2007GB003154 (2008).
40. Kwon, E. Y. & Primeau, F. Optimization and sensitivity study of a biogeochemistry ocean model using an implicit solver and *in situ* phosphate data. *Glob. Biogeochem. Cycles* **20,** doi:10.1029/2005GB002631 (2006).